

Correlation functions in first-order phase transitions

V. Garrido and D. Crespo*

Departament de Física Aplicada, Universitat Politècnica de Catalunya, Campus Nord UPC, Mòdul B4, 08034, Barcelona, Spain

(Received 4 April 1997)

Most of the physical properties of systems underlying first-order phase transitions can be obtained from the spatial correlation functions. In this paper, we obtain expressions that allow us to calculate all the correlation functions from the droplet size distribution. Nucleation and growth kinetics is considered, and exact solutions are obtained for the case of isotropic growth by using self-similarity properties. The calculation is performed by using the particle size distribution obtained by a recently developed model (populational Kolmogorov-Johnson-Mehl-Avrami model). Since this model is less restrictive than that used in previously existing theories, the result is that the correlation functions can be obtained for any dependence of the kinetic parameters. The validity of the method is tested by comparison with the exact correlation functions, which had been obtained in the available cases by the time-cone method. Finally, the correlation functions corresponding to the microstructure developed in partitioning transformations are obtained. [S1063-651X(97)12209-7]

PACS number(s): 05.70.Fh, 05.70.Ln, 82.20.Mj, 81.30.-t

I. INTRODUCTION

Solid-state transformations usually occur by nucleation and subsequent growth of particles in a volume or at an interface. The reaction kinetics may be interface controlled, as in the case of recrystallization of metals, or diffusion limited, as in the case of primary crystallizations. For both types of kinetics, the transformation may be analyzed by the theory of nucleation and growth processes developed in the 1930s by Kolmogorov, Johnson and Mehl, and Avrami (KJMA) [1–5]. Recently, and after some questioning, the theory has been rederived requiring only the hypothesis of random nucleation [6,7]. The theory is able to evaluate the time dependence of the transformed fraction during the transformation from the knowledge of the kinetic magnitudes, namely, nucleation rate I and growth rate G . An extension of the theory based on the same hypotheses as KJMA plus a mean field hypothesis has been derived by Crespo and Pradell [8] to allow the evaluation of the particle size population as a function of time, which is based on the knowledge, as in KJMA, of the kinetic magnitudes $I(t)$, $G(t)$ and considers the size of the nuclei while formed. The determination of the resulting particle size distributions from a primary crystallization is of highest interest in obtaining good physical properties by means of controlling the density and sizes of the particles, i.e., nanocrystalline materials obtained by primary crystallization of metallic glasses. The particle size distributions have already been obtained for interface and diffusion controlled growth processes [8,9], and for the case of a primary precipitation during annealing of a glassy alloy resulting in a nanocrystalline structure [10]. We will call this model “populational KJMA.”

Furthermore, the experimental evaluation of particle size distributions is also of highest interest. Several techniques exist for the evaluation of microstructures; namely, scanning and transmission electron microscopy (SEM and TEM), and small angle x-ray and neutron diffraction (SAXS and

SANS). While SEM and TEM pictures give directly approximated particle size distributions, SAXS and SANS give an indirect measure by means of the Fourier transform of the autocorrelation function corresponding to the particle size distribution [11]. Moreover, macroscopical properties of the materials are also related to the spatial correlation functions. Therefore, the evaluation of the correlation functions from the particle size distributions is becoming of major interest.

An elegant theory that gives exact correlation functions for a first order phase transition in a p degenerated system was developed nearly ten years ago by Ohta *et al.* [12], and is known as the time-cone method. However, the hypothesis under which the method is deduced heavily restricts its practical applicability to real systems. For the particular case of a nondegenerated system, $p=1$, Sekimoto [13–15] has derived a formal solution that gives the particle size populations and the correlation functions. However, the particular case $p=1$ is not extensive to higher degrees of degeneration ($p>1$). Furthermore, there is no expression able to evaluate the particle size distributions from such correlation functions.

The model for evaluating grain size populations in a first order phase transition, “populational KJMA,” was developed for a completely degenerated system ($p\rightarrow\infty$). However, the correlation functions of a nondegenerated ($p=1$) and partially degenerated ($1<p<\infty$) systems can be expressed in terms of the correlation functions of the completely degenerated ($p\rightarrow\infty$) system, as will be demonstrated in the present paper. On the other hand, the model is less restrictive than the time-cone method, and allows evaluation of correlation functions for nontrivial kinetics where the time-cone method cannot be applied, i.e., $I(x,t)$, $G(x,r,t)$, where t is the time, x is the transformed fraction at time t , and r is the individual radius of the growing droplets.

The object of the present paper is the evaluation of the correlation functions from a given particle size distribution, which may be obtained either by using the “populational KJMA” method or by any other calculation or experimental method. Correlation functions are calculated for the p -JM model (p degenerated Johnson-Mehl with $I=\text{const}$,

*Electronic address: crespo@benard.upc.es

$G=\text{const}$) and p -cell [p degenerated with $I=I_0\delta(t)$ and $G=\text{const}$] in two and three dimensions, and the results reproduce exactly the correlation functions obtained by the time-cone method. Correlation functions corresponding to a $I=\text{const}$ and diffusion limited growth with hard and soft impingement, $I=I_0$ and $G=G(r,x)$, characteristic of a primary crystallization, have also been calculated. In this case the time-cone method cannot be applied, and therefore the obtained correlation functions cannot be compared.

II. GENERALIZED CORRELATION FUNCTIONS

A. Theory

The correlation functions are intimately related to the phase structure developed during the phase transition. Generalizing the conventions used by Sekimoto [13,16] and Ohta *et al.* [12] we can distinguish between droplets, domains, phases, and total transformed phase, according to the following definitions.

(1) ‘‘Droplet’’ at time t (G): the bounded region that comes from the i th center of nucleation. This region is characterized by its shape, which is specified by its index α . It also belongs to one of the transformed phases, k . The D -dimensional vector $\mathbf{r}_{\alpha i}$ distinguishes the location of this region. Here we mean by the location $\mathbf{r}_{\alpha i}$ of the region $W_{k\alpha}(\mathbf{r}_{\alpha i})$ the location of the representative point $P_{k\alpha i}$, the nucleation center, which we fix for respective (αi) relatively to the region $W_{k\alpha}$:

$$(G)_{k\alpha i} = W_{k\alpha}(\mathbf{r}_{\alpha i}). \quad (2.1)$$

(2) ‘‘Domain’’ at time t (D): the union of the self-similar bounded regions $W_{k\alpha}(\mathbf{r}_{\alpha i})$ with common shape α at time t :

$$(D)_{k\alpha} = \bigcup_i W_{k\alpha}(\mathbf{r}_{\alpha i}). \quad (2.2)$$

(3) ‘‘Phase’’ at time t (P): the union of all the bounded regions $\{W_{k\alpha}(\mathbf{r}_{\alpha i})\}$ at time t with common k :

$$(P)_k = \bigcup_{\alpha} \bigcup_i W_{k\alpha}(\mathbf{r}_{\alpha i}). \quad (2.3)$$

(4) ‘‘Transformed phase’’ at time t (TP): the union of all the phases:

$$(\text{TP}) = \bigcup_k \bigcup_{\alpha} \bigcup_i W_{k\alpha}(\mathbf{r}_{\alpha i}). \quad (2.4)$$

In order to study the correlation functions, it is necessary to characterize the phases. Previous work performed by Ohta *et al.* [12] by using the time-cone method was developed over a system exhibiting the following properties: (i) The order parameter has a p -simplex symmetry where p may be infinite. Near the transition point, the order parameter has a unique value that is taken to be zero and corresponds to a stable disordered state. Trespassing the transition point the p phases are perfectly degenerate so that interfaces dividing any two of the p stable phases are equivalent. p ‘‘colors’’ are assigned to the p phases. (ii) By an external variable, usually temperature, the system is quenched from the disordered state with color ‘‘0’’ to the ordered phases. Once the transition point is trespassed, the stable ordered droplets nucleate randomly and grow in the matrix ‘‘0,’’ which is now meta-

stable. This randomness enables us to use the Poisson distribution for nucleation events. Each droplet is assigned to one of the colors from ‘‘1’’ to ‘‘ p .’’ (iii) An ordered droplet cannot shrink. Furthermore, the normal velocity of a growing droplet front is not an increasing function of time and is independent of the color ‘‘ i .’’ The finiteness of a critical radius is ignored; its existence effectively violates this condition. A spatially anisotropic growth is allowed. (iv) The velocity of a moving droplet front is not affected by the environment except by collision of the fronts. It is assumed that the anisotropy of the velocity is not strong enough for the velocity to be well defined at any instant near the intersection of two droplet fronts. When two droplets collide with each other the droplet front between them disappears if their colors are the same. If their colors are different both droplets cease to grow at that point so that a static interface is constructed. Thus, the system is eventually occupied by frozen ordered droplets. A coarse-grained picture is adopted so that the width of interfaces is infinitesimal.

In this model the nucleation rate $I(t)$ is introduced in such a way that $I(t)dt$ droplets nucleate per unit volume in the matrix ‘‘0’’ in the time interval between t and $t+dt$. Because of the perfect degeneracy of p stable phases, the nucleation rate of a droplet with color ‘‘ i ’’ is independent of ‘‘ i ’’ and is equal to $I(t)/p$.

It is important to note that some of these restrictions are specific to the time-cone method and are not related to the definition of the correlation functions themselves. Therefore, if the information about droplet size distribution is available from any alternative means, either experimental or theoretical, the correlation functions can be exactly calculated, as will be shown later. In particular, this allows us to overcome three of the above restrictions: (1) It is possible to study systems where the normal velocity of a growing droplet front is an increasing function of time. (2) It is possible to take into account the finiteness of the critical radius. (3) It is possible to study systems where the velocity of a moving droplet front is affected by the environment and not only by collision; for example, in diffusion controlled growth with hard or soft impingement.

In the following, we derive the expressions for the correlations functions. First, we recall the definitions and some of their properties. Then we demonstrate that any of the correlation functions may be obtained as a function of the droplet autocorrelation function. Finally, an expression for calculating the droplet autocorrelation function as a function of the particle size distribution is presented.

In order to represent the phase structure, it is convenient to introduce the following two-valued function:

$$g_i(\mathbf{r}, t) = \begin{cases} 1, & \text{if } \mathbf{r} \text{ belongs to a droplet of } i\text{th phase} \\ & \text{at time } t \\ 0, & \text{otherwise.} \end{cases} \quad (2.5)$$

Since any spatial point belongs to one of the phases ‘‘0’’ to ‘‘ p ,’’ it should have the following identity:

$$1 = \sum_{i=0}^p g_i(\mathbf{r}, t). \quad (2.6)$$

Then it is easily shown that

$$\phi_i(t) = \langle g_i(\mathbf{r}, t) \rangle = \frac{1}{p} [1 - \phi_0(t)] = \phi_1(t), \quad (2.7)$$

where $\phi_i(t)$ is the volume fraction of the phase with color “ i ,” and $\phi_0(t)$ is the volume fraction of the matrix “0.” In other words, $\phi_i(t)$ is the probability of finding a point at time t in a phase “ i ,” and $\phi_0(t)$ is the probability of finding a point at time t in a matrix “0.”

The following is also obtained [13,16]:

$$\begin{aligned} \phi_0(t) &= \exp[-\Delta^{(1)}(t)], \\ \Delta^{(1)}(t) &= \int_0^t d\tau I(\tau) V(t-\tau), \end{aligned} \quad (2.8)$$

where $\Delta^{(1)}(t)$ is the “extended volume,” and $V_1(t-\tau)$ is, at time t , the volume of a droplet nucleated at time τ .

The correlation functions are defined as

$$\begin{aligned} G_0(\mathbf{r}-\mathbf{r}', t) &= \langle g_0(\mathbf{r}, t) g_0(\mathbf{r}', t) \rangle, \\ G_1(\mathbf{r}-\mathbf{r}', t) &= \langle g_i(\mathbf{r}, t) g_i(\mathbf{r}', t) \rangle, \end{aligned} \quad (2.9)$$

$$H_0(\mathbf{r}-\mathbf{r}', t) = \langle g_0(\mathbf{r}, t) g_i(\mathbf{r}', t) \rangle,$$

$$H_1(\mathbf{r}-\mathbf{r}', t) = \langle g_i(\mathbf{r}, t) g_j(\mathbf{r}', t) \rangle, \quad i \neq j$$

where the angular brackets mean the average over all possible sets of nucleation and growth behaviors. Taking $\mathbf{r}'=0$ for simplicity, and without loss of generality, (1) $G_0(\mathbf{r}, t)$ is the probability of finding, at time t , two points separated by a distance \mathbf{r} in the matrix “0.” (2) $G_1(\mathbf{r}, t)$ is the probability of finding, at time t , two points separated by a distance \mathbf{r} in the same phase “ i .” (3) $H_0(\mathbf{r}, t)$ is the probability of finding, at time t , two points separated by a distance \mathbf{r} , one in the matrix “0” and the other in the phase “ i .” (4) $H_1(\mathbf{r}, t)$ is the probability of finding, at time t , two points separated by a distance \mathbf{r} , one in the phase “ i ” and the other in the phase “ j ,” where “ i ” and “ j ” represent different phases.

However, noting the identity (2.6), the above four functions are not mutually independent. In fact, they satisfy the following relations

$$1 = \underbrace{G_0(\mathbf{r}, t) + pH_0(\mathbf{r}, t)}_{\phi_0(t)} + \underbrace{pH_0(\mathbf{r}, t) + p(p-1)H_1(\mathbf{r}, t) + pG_1(\mathbf{r}, t)}_{1-\phi_0(t)} \quad (2.10)$$

$$H_0(\mathbf{r}, t) = \frac{1}{p} [\phi_0(t) - G_0(\mathbf{r}, t)],$$

$$H_1(\mathbf{r}, t) = \frac{1}{p(p-1)} [C_0(\mathbf{r}, t) - pG_1(\mathbf{r}, t)], \quad (2.11)$$

where

$$C_0(\mathbf{r}, t) = 1 - 2\phi_0(t) + G_0(\mathbf{r}, t). \quad (2.12)$$

Thus, without loss of generality, we can choose $\phi_0(t)$, $G_0(\mathbf{r}, t)$, and $G_1(\mathbf{r}, t)$ as the basic quantities. The next step is to calculate $G_0(\mathbf{r}, t)$ and $G_1(\mathbf{r}, t)$. These quantities, given Eq. (2.12), are evaluated as

$$G_0(\mathbf{r}, t) = C_0(\mathbf{r}, t) + 2\phi_0(t) - 1, \quad (2.13)$$

$$G_1(\mathbf{r}, t) = \frac{1}{p^2} C_0(\mathbf{r}, t) + \frac{p-1}{p^2} C_1(\mathbf{r}, t).$$

Here, $C_1(\mathbf{r}, t)$ is the probability of finding, at time t , two points separated by a distance \mathbf{r} in the same droplet into the whole transformed phase. In other words, it is the droplet transformed phase autocorrelation function averaged for all the droplets of the transformed phase. The difference between $G_1(\mathbf{r}, t)$ and $C_1(\mathbf{r}, t)$ is that $G_1(\mathbf{r}, t)$ is taken into account as well as the connected and the nonconnected droplets of the transformed phase, while $C_1(\mathbf{r}, t)$ accounts only for

individual droplets. In this sense, it is interesting to note that using Eqs. (2.11), (2.12) and (2.13) we can rewrite $G_1(\mathbf{r}, t)$ and $H_1(\mathbf{r}, t)$:

$$G_1(\mathbf{r}, t) = H_1(\mathbf{r}, t) + \frac{C_1(\mathbf{r}, t)}{p}, \quad (2.14)$$

$$H_1(\mathbf{r}, t) = \frac{C_0(\mathbf{r}, t) - C_1(\mathbf{r}, t)}{p^2},$$

where the term $G_1(\mathbf{r}, t)$ involves the nonconnected droplets in the transformed phase. This is clear from the deduction of $G_1(\mathbf{r}, t)$ in the time-cone method where two mechanisms are used to build $G_1(\mathbf{r}, t)$ independently of the phases, the first accounting for the covering of the two points from a single nucleation center, and the second accounting for the covering of the two points from two different nucleation centers.

Taking into account the expressions given in Eqs. (2.10), (2.11), and (2.12) we can write

$$G_0(\mathbf{r}, t) = \phi_0(t) - pH_0(\mathbf{r}, t),$$

$$\begin{aligned} C_0(\mathbf{r}, t) &= [1 - \phi_0(t)] - pH_0(\mathbf{r}, t) = p(p-1)H_1(\mathbf{r}, t) \\ &+ pG_1(\mathbf{r}, t) \end{aligned} \quad (2.15)$$

TABLE I. Asymptotic behavior of the correlation functions.

		$\phi_0(0)=1$	$\phi_0(\infty)=0$
		$\phi_1(0)=0$	$\phi_1(\infty)=p^{-1}$
$G_0(0,t)=\phi_0(t)$	$G_0(\infty,t)=\phi_0^2(t)$	$G_0(r,0)=1$	$G_0(r,\infty)=0$
$G_1(0,t)=\phi_1(t)$	$G_1(\infty,t)=\phi_1^2(t)$	$G_1(r,0)=0$	$G_1(r,\infty)=p^{-2}+(p-1)p^{-2} C_1(r,\infty)$
$H_0(0,t)=0$	$H_0(\infty,t)=\phi_0(t) \phi_1(t)$	$H_0(r,0)=0$	$H_0(r,\infty)=0$
$H_1(0,t)=0$	$H_1(\infty,t)=\phi_1^2(t)$	$H_1(r,0)=0$	$H_1(r,\infty)=p^{-2}[1-C_1(r,\infty)]$
$C_0(0,t)=1-\phi_0(t)$	$C_0(\infty,t)=[1-\phi_0(t)]^2$	$C_0(r,0)=0$	$C_0(r,\infty)=1$
$C_1(0,t)=1-\phi_0(t)$	$C_1(\infty,t)=0$	$C_1(r,0)=0$	$C_1(r,\infty)$

and thus we can interpret $C_0(\mathbf{r},t)$ as the global correlation function of the whole transformed phase without interaction with the nontransformed phase.

We can now define the problem we wish to solve. Equations (2.9)–(2.15) are formal expressions calculable by the time-cone method in trivial kinetics, but their computation is extremely difficult in nontrivial kinetics. Therefore we need another point of view to solve the problem in practical situations. Our approach employs the evaluation of the droplet size distribution and the reformulation of the correlation functions by using only the droplet autocorrelation function.

First, let us study the asymptotic behavior of the correlation functions. Since $g_i(\mathbf{r},t)$ takes the value of either zero or unity $G_0(\mathbf{r},t)$, $G_1(\mathbf{r},t)$, and $H_0(\mathbf{r},t)$, $H_1(\mathbf{r},t)$ approach $\phi_0(t)$, $\phi_1(t)$, 0, and 0, respectively, as $r \rightarrow 0$. As $r \rightarrow \infty$ correlation should disappear since the nucleation events are random, so that $G_0(\mathbf{r},t)=\phi_0^2(t)$, $G_1(\mathbf{r},t)=\phi_1^2(t)$, $H_0(\mathbf{r},t)=\phi_0(t) \phi_1(t)$, and $H_1(\mathbf{r},t)=\phi_1^2(t)$. These behaviors are summarized in Table I. The limit values of these functions are also shown in Table II.

From the study of the asymptotic behavior of the correlation functions and its limit values, we can arrive at several considerations:

(1) It is important to note that when t is sufficiently large, $C_0(\mathbf{r},t)$ approaches unity so that $G_1(\mathbf{r},\infty)=1/p^2+(p-1)C_1(\mathbf{r},\infty)/p^2$ for $p>1$. On the other hand, in the limit $p \rightarrow \infty$ there is $G_1(\mathbf{r},t)=C_1(\mathbf{r},t)/p$. This implies that the asymptotic structure function of the area occupied by ‘‘1’’ phases, the transformed phase, which is intricately interconnected for small values of p , is simply given by the structure function of an isolated ‘‘1’’ phase, which appears for $p \rightarrow \infty$. This means that if there is any way of obtaining the structure of the transformed phase in the limit $p \rightarrow \infty$, it is always possible to obtain the structure functions for any value of p ; in other words, the structure of the transformed phase in the limit $p \rightarrow \infty$ contains all the information about the structure of all the cases of finite p .

(2) $G_0(\mathbf{r},t)$, $C_0(\mathbf{r},t)$, and $C_1(\mathbf{r},t)$ are independent of p .

(3) All the curves of these magnitudes grow with t except

TABLE II. Limit values of the correlation functions.

$G_0(0,0)=1$	$G_0(\infty,0)=1$	$G_0(0,\infty)=0$	$G_0(\infty,\infty)=0$
$G_1(0,0)=0$	$G_1(\infty,0)=0$	$G_1(0,\infty)=p^{-1}$	$G_1(\infty,\infty)=p^{-2}$
$H_0(0,0)=0$	$H_0(\infty,0)=0$	$H_0(0,\infty)=0$	$H_0(\infty,\infty)=0$
$H_1(0,0)=0$	$H_1(\infty,0)=0$	$H_1(0,\infty)=0$	$H_1(\infty,\infty)=p^{-2}$
$C_0(0,0)=0$	$C_0(\infty,0)=1$	$C_0(0,\infty)=1$	$C_0(\infty,\infty)=1$
$C_1(0,0)=0$	$C_1(\infty,0)=0$	$C_1(0,\infty)=1$	$C_1(\infty,\infty)=0$

$G_0(\mathbf{r},t)$, which decreases, and $H_0(\mathbf{r},t)$, which grows until $\phi_0(t)=\phi_1(t)$ and decreases afterwards.

From Eq. (2.9) and the general definitions of $\phi_0(t)$ and $\phi_i(t)$,

$$\phi_0(t)=\langle g_0(\mathbf{r},t) \rangle,$$

$$\phi_i(t)=\langle g_i(\mathbf{r},t) \rangle, \quad (2.16)$$

$$H_0(\mathbf{r},t)=\langle g_0(\mathbf{r},t)g_i(\mathbf{0},t) \rangle.$$

We can factorize $H_0(\mathbf{r},t)$ as

$$H_0(\mathbf{r},t)=\phi_0(t)\phi_1(t)\left[1-\frac{1}{[1-\phi_0(t)]^2}\times\sum_i^p\phi_i(t)[1-\phi_0(t)]h_{0i}(\mathbf{r})\right], \quad (2.17)$$

where $h_{0i}(\mathbf{r})$ is the function that accounts for the interaction between transformed and untransformed phases, and must fulfill $h_{0i}(0)=1$ and $h_{0i}(\infty)=0$.

Thus, we can define the new function $F(\mathbf{r},t)$ as

$$F(\mathbf{r},t)=\frac{1}{[1-\phi_0(t)]^2}\sum_i^p\phi_i(t)[1-\phi_0(t)]h_{0i}(\mathbf{r}), \quad (2.18)$$

where the temporal and spatial dependencies have been separated.

We can factorize $H_1(\mathbf{r},t)$ in the same way. $H_1(\mathbf{r},t)$ gives the probability of finding, at time t , two points belonging to two different transformed phases at a distance \mathbf{r} . So it must be a quadratic function of the volume occupied by the transformed phases, and can be written as

$$H_1(\mathbf{r},t)=\frac{p}{(p-1)}\phi_1^2(t)\left[1-\frac{1}{[1-\phi_0(t)]^2}\times\sum_i^p\sum_{j\neq i}^p\phi_i(t)\phi_j(t)h_{ij}(\mathbf{r})\right], \quad (2.19)$$

where $h_{ij}(\mathbf{r})$ is the function that accounts for the interaction between phases, and must fulfill $h_{ij}(0)=1$ and $h_{ij}(\infty)=0$.

When $p \rightarrow \infty$ we get

$$H_1(\mathbf{r},t)=\phi_1^2(t)\left[1-\frac{1}{[1-\phi_0(t)]^2}\sum_i^p\sum_j^p\phi_i(t)\phi_j(t)h_{ij}(\mathbf{r})\right]. \quad (2.20)$$

Here we will identify the second term with the above defined $F(\mathbf{r}, t)$, that is,

$$F(\mathbf{r}, t) = \frac{1}{[1 - \phi_0(t)]^2} \sum_i^p \sum_j^p \phi_i(t) \phi_j(t) h_{ij}(\mathbf{r}), \quad (2.21)$$

which implies that

$$h_{0i}(r) = \frac{1}{[1 - \phi_0(t)]} \sum_j^p \phi_j(t) h_{ij}(r). \quad (2.22)$$

Summarizing, we have deduced expressions for $H_0(\mathbf{r}, t)$, $H_1(\mathbf{r}, t)$, namely,

$$\begin{aligned} H_0(\mathbf{r}, t) &= \phi_0(t) \phi_1(t) [1 - F(\mathbf{r}, t)], \\ H_1(\mathbf{r}, t) &= \phi_1^2(t) [1 - F(\mathbf{r}, t)] \end{aligned} \quad (2.23)$$

as a function of $F(\mathbf{r}, t)$, of which we have two different functional forms (2.18) and (2.21) related by Eq. (2.22).

Replacing Eq. (2.23) in Eqs. (2.11), (2.12), and (2.13) we obtain

$$\begin{aligned} G_0(\mathbf{r}, t) &= \phi_0(t) \{ \phi_0(t) + F(\mathbf{r}, t) [1 - \phi_0(t)] \}, \\ G_1(\mathbf{r}, t) &= \phi_1(t) \{ \phi_1(t) + F(\mathbf{r}, t) [1 - \phi_1(t)] \}, \\ C_0(\mathbf{r}, t) &= [1 - \phi_0(t)] \{ [1 - \phi_0(t)] [1 - F(\mathbf{r}, t)] \}, \\ C_1(\mathbf{r}, t) &= [1 - \phi_0(t)] F(\mathbf{r}, t). \end{aligned} \quad (2.24)$$

In these equations we can observe the right asymptotic behaviors of all the correlation functions. From the last equation we can write all the correlation functions as a function of $\phi_0(t)$, $C_1(\mathbf{r}, t)$, and p :

$$\begin{aligned} G_0(\mathbf{r}, t) &= \phi_0^2(t) + \phi_0(t) C_1(\mathbf{r}, t), \\ G_1(\mathbf{r}, t) &= \frac{1}{p^2} \{ [1 - \phi_0(t)]^2 + [\phi_0(t) + (p-1)] C_1(\mathbf{r}, t) \}, \\ H_0(\mathbf{r}, t) &= \frac{1}{p} \phi_0(t) \{ [1 - \phi_0(t)] - C_1(\mathbf{r}, t) \}, \\ H_1(\mathbf{r}, t) &= \frac{1}{p^2} [1 - \phi_0(t)] \{ [1 - \phi_0(t)] - C_1(\mathbf{r}, t) \}, \\ C_0(\mathbf{r}, t) &= [1 - \phi_0(t)]^2 + \phi_0(t) C_1(\mathbf{r}, t). \end{aligned} \quad (2.25)$$

Equations (2.23), (2.24), and (2.25) show that the problem of determining all the correlation functions has been reduced to the determination of the unknown function $F(\mathbf{r}, t)$. To interpret $F(\mathbf{r}, t)$ we will use the properties of $C_1(\mathbf{r}, t)$. As previously stated, $C_1(\mathbf{r}, t)$ is the probability of finding, at time t , two points separated by a distance \mathbf{r} in the same droplet of the transformed volume; in Eq. (2.24) we can see that $C_1(\mathbf{r}, t)$ is the probability of finding a point belonging to the transformed phase times $F(\mathbf{r}, t)$, so $F(\mathbf{r}, t)$ must be the system global averaged autocorrelation function.

From this concept we can develop Eq. (2.24) to obtain the general expression that gives $C_1(\mathbf{r}, t)$ as a function of the

droplet shape-size distribution function, which is supposed to be previously known. We can define $F(\mathbf{r}, t)$ as

$$F(\mathbf{r}, t) = \frac{1}{N} \sum_i^N f_i(\mathbf{r}, t) = \frac{1}{1 - \phi_0(t)} \sum_i^N \phi_i(t) f_i(\mathbf{r}, t), \quad (2.26)$$

where N is the total number of droplets, and $f(\mathbf{r}, t)$ is the droplet autocorrelation function at time t . We can take advantage of the self-similar properties of the members of the same domain, which we can extend across different phases. Thus,

$$\begin{aligned} F(\mathbf{r}, t) &= \frac{1}{N} \sum_k \sum_\alpha \sum_\beta N_{k\alpha\beta}(t) f_{\alpha\beta}(\mathbf{r}) \\ &= \frac{1}{1 - \phi_0(t)} \sum_k \sum_\alpha \sum_\beta N_{k\alpha\beta}(t) \phi_k(t) f_{\alpha\beta}(\mathbf{r}), \end{aligned} \quad (2.27)$$

where k labels the phases, α labels the domains of each phase, β labels the different sizes of the droplets into a specific domain, and $N_{k\alpha\beta}$ accounts for the number of droplets of the same size β in a given domain α of a given phase k .

Note that the last equation has the functional form of Eq. (2.18), and $h_{0i}(r)$ can be interpreted as $f_{\alpha\beta}(r)$, the individual autocorrelation function. Moreover, it is important to note that in the last equation the time dependence is assumed by $N_{k\alpha\beta}$, the droplet size-shape distribution function, while $f_{\alpha\beta}$ notices the individual droplet autocorrelation function of shape α and size β .

Reordering the sums and multiplying the two sides of the last equation by the transformed phase, $[1 - \phi_0(t)]$, we obtain

$$[1 - \phi_0(t)] F(\mathbf{r}, t) = \sum_\beta \sum_\alpha \sum_k \frac{N_{k\alpha\beta}(t)}{N} [1 - \phi_0(t)] f_{\alpha\beta}(\mathbf{r}). \quad (2.28)$$

We can interpret $\sum_k N_{k\alpha\beta}(t)/N$ as the probability of finding droplets of $(\alpha\beta)$ type in the transformed phase at time t . Also, we can interpret $\sum_k [N_{k\alpha\beta}(t)/N] [1 - \phi_0(t)]$ as the nD volume (n -dimensional volume) fraction corresponding to the droplets of $(\alpha\beta)$ type at time t .

Using the last equation of (2.24), we obtain

$$C_1(\mathbf{r}, t) = \sum_\beta \sum_\alpha \left(\frac{V_{\alpha\beta}(t)}{V} \right) f_{\alpha\beta}(\mathbf{r}), \quad (2.29)$$

where $V_{\alpha\beta}(t)$ is the nD volume occupied by the droplets of $(\alpha\beta)$ type at time t , and V is the nD volume of the whole system under consideration.

Developing $V_{\alpha\beta}(t)$ as a function of the number of droplets of $(\alpha\beta)$ type, $N_{\alpha\beta}$, and the nD volume of each droplet, $\bar{V}_{\alpha\beta}$, we have

$$C_1(\mathbf{r}, t) = \sum_\beta \sum_\alpha \frac{N_{\alpha\beta}(t) \bar{V}_{\alpha\beta}}{V} f_{\alpha\beta}(\mathbf{r}), \quad (2.30)$$

and thus

$$C_1(\mathbf{r}, t) = \sum_{\beta} \sum_{\alpha} n_{\alpha\beta}(t) \bar{V}_{\alpha\beta} f_{\alpha\beta}(\mathbf{r}), \quad (2.31)$$

where $n_{\alpha\beta}(t)$ is the nD density of the droplets of $(\alpha\beta)$ type at time t .

Computation of $f_{\alpha\beta}(\mathbf{r})$ is significantly simplified by recalling that $\bar{V}_{\alpha\beta} f_{\alpha\beta}(\mathbf{r})$ is the theoretical excluded nD volume [5,13] of two similar droplets with a separation between centers of \mathbf{r} . A greater advantage is gained if we recall that it is only necessary to calculate one typical droplet autocorrelation function by domain, since all the droplets of one domain are self-similar, of the same shape, and their autocorrelation functions are scalable. Thus, defining

$$\tilde{f}_{\alpha}\left(\frac{\mathbf{r}}{1}\right) = f_{\alpha 1}(\mathbf{r}) \quad (2.32)$$

as the droplet autocorrelation function of a unit length droplet, we have

$$f_{\alpha\beta}(\mathbf{r}) = \tilde{f}_{\alpha}\left(\frac{\mathbf{r}}{r_{\beta}}\right) \quad (2.33)$$

and the final expression of $C_1(\mathbf{r}, t)$ becomes

$$C_1(\mathbf{r}, t) = \sum_{\beta} \sum_{\alpha} n_{\alpha\beta}(t) \bar{V}_{\alpha\beta} \tilde{f}_{\alpha}\left(\frac{\mathbf{r}}{r_{\beta}}\right). \quad (2.34)$$

Equation (2.34) allows one to determine $C_1(\mathbf{r}, t)$ exactly and, as we have shown, the rest of the correlation functions, whether the exact droplet size-shape distribution is known, because no approximations have been used in its derivation.

B. Application to isotropic growth

Equation (2.34) is a formal expression. It can be calculated if the shape and space orientation of all grains are known, but this is in fact impossible in practical situations due to impingement between growing grains. Moreover, an infinite number of droplet shapes exists, corresponding to impingement between two, three, or more grains.

Nevertheless, we can calculate a first approximation to $C_1(\mathbf{r}, t)$, in the case of isotropic growth, neglecting impingement and assuming that grains are perfectly nD spherical. It is referred to as $C_1^0(r, t)$, defined by

$$C_1^0(r, t) = \sum_{\beta} n_{\beta}(t) \bar{V}_{\beta} \tilde{f}_0\left(\frac{r}{r_{\beta}}\right), \quad (2.35)$$

where $\tilde{f}_0(r/r_{\beta})$ is the autocorrelation function of an nD sphere given by

$$\tilde{f}_0\left(\frac{r}{r_i}\right) = \left[1 - \frac{3}{4}\left(\frac{r}{r_i}\right) + \frac{1}{16}\left(\frac{r}{r_i}\right)^3\right] \Theta(2r_i - r) \quad (2.36)$$

for three dimensions and

$$\tilde{f}_0\left(\frac{r}{r_i}\right) = \left\{1 - \frac{r}{\pi r_i} \left[1 - \left(\frac{r}{2r_i}\right)^2\right]^{1/2} - \frac{2}{\pi} \arcsin\left(\frac{r}{2r_i}\right)\right\} \times \Theta(2r_i - r) \quad (2.37)$$

for two dimensions, and Θ is the Heaviside function. It is important to note that we have chosen as the initial droplet autocorrelation function the one corresponding to the more compact geometrical shape in its respective dimensions. The relation between the nD volume and the radius of the droplet is obviously

$$\bar{V}_{\beta} = \frac{2\pi^{D/2}}{d\Gamma(D/2)} r_{\beta}^D. \quad (2.38)$$

Thus $C_1^0(r, t)$ gives the autocorrelation function of a system of nonoverlapped spheres occupying the transformed volume at any time t . In the limit $t \rightarrow \infty$, the transformed volume fills the whole space, and then the topology described by $C_1^0(r, t)$ is impossible. However, the transformed fraction is conserved by $C_1^0(r, t)$, because it can be easily proved that

$$\int_0^{\infty} dr \frac{2\pi^{D/2}}{\Gamma(D/2)} r^{(D-1)} C_1^0(r, t) = \frac{[1 - \phi_0(t)]^2}{n(t)} = [1 - \phi_0(t)] \langle V(t) \rangle, \quad (2.39)$$

where $n(t)$ and $\langle V(t) \rangle$ are respectively the total nD density of droplets (number of droplets by unit nD volume) and the average nD volume of a droplet at time t . Therefore, we see that the calculated $C_1^0(r, t)$, without considering impingement, is the first order averaged autocorrelation function or, in other words, the autocorrelation function of an ‘‘average droplet.’’

Looking again at $C_1^0(r, t)$, we can easily see that it is not the autocorrelation function of an nD sphere. It could only be this in the case where all the grains were nD spheres of the same radius, that is, $n_{\beta}(r, t) = n_0(t) \delta(r - r_0)$. Moreover, since an nD spherical object is the most geometrically compact object, $C_1^0(r, t)$ is sure to extend to a distance larger than the autocorrelation function of an nD sphere of the same nD volume. That is to say, the average droplet is less compact than a nD sphere, but preserves the nD -spherical symmetry.

However, in order to obtain the actual $C_1(r, t)$ we need an additional hypothesis. We will first characterize true droplets by their *effective radius*, defined by

$$r_{\beta} = \left(\frac{D\Gamma(D/2)}{2\pi^{D/2}} \bar{V}_{\beta}\right)^{1/D}, \quad (2.40)$$

corresponding to the radius of an nD sphere of the same volume. Then we will use the fact that the shape distribution of grain populations characterized by different effective radius r_{β} are self-similar. In other words, the shape distribution of all the grains having the same volume is independent of the value of this volume. Consequently, the autocorrelation functions of these populations are also self-similar, and are scaled by a characteristic length that is chosen as the effective radius. Finally, we can assume that $C_1^0(r, t)$ is represen-

tative of all of them, because it corresponds to the autocorrelation function of the ‘‘average spherical droplet.’’ Its radius $L(t)$, defined in the same way as before,

$$L(t) = \left(\frac{d\Gamma(D/2)}{2\pi^{D/2}} \langle V(t) \rangle \right)^{1/D}, \quad (2.41)$$

will be used as the corresponding scaling length.

Therefore, the expression for $C_1(r, t)$ is obtained by replacing $\tilde{f}_0(r/r_\beta)$ by $C_1^0(rL/r_\gamma)$ in the definition of $C_1^0(r, t)$ given by Eq. (2.35):

$$\begin{aligned} C_1(r, t) &= \sum_\gamma n_\gamma \bar{V}_\gamma \left[\frac{1}{1 - \phi_0(t)} C_1^0\left(\frac{rL}{r_\gamma}\right) \right] \\ &= \frac{1}{1 - \phi_0(t)} \sum_\gamma \sum_\beta n_\gamma n_\beta \bar{V}_\gamma \bar{V}_\beta \tilde{f}_0\left(\frac{rL}{r_\beta r_\gamma}\right) \\ &= \frac{1}{1 - \phi_0(t)} \sum_\gamma \sum_\beta \phi_\gamma \phi_\beta \tilde{f}_0\left(\frac{rL}{r_\beta r_\gamma}\right), \end{aligned} \quad (2.42)$$

which has the functional form required by Eq. (2.21), and where we can identify the transformation given by Eq. (2.22), affected by a scale factor. This equation takes into account the impingement throughout the interaction between populations, resulting in non- nD -spherical droplets.

The behavior of $C_1(r, t)$ is slightly different from the $C_1^0(r, t)$ due to the fact that we have built nonspherical droplet autocorrelation functions. Thus, (1) $C_1^0(r, t)$ extends to $r = 2R_{\max}$ while $C_1(r, t)$ extends to $r = 2R_{\max}^2/L > 2R_{\max}$, R_{\max} being the largest droplet radius of the population. (2) $C_1(r, t) < C_1^0(r, t)$ for $r \rightarrow 0$.

The physical reason for this behavior is that the built nonspherical autocorrelation function is less compact than the original one, and consequently its tail extends further. Then, the behavior obtained for $r \rightarrow 0$ is due to the conservation of the transformed volume, expressed by Eq. (2.39), and the fact that $C_1(r, t)$ and $C_1^0(r, t)$ are monotonically decreasing functions.

Equation (2.42) is postulated from the above cited plausibility arguments, that is, it has the functional form required by Eqs. (2.18) and (2.21) and takes into account the isotropy considerations. Moreover, in its deduction no approximations have been made and, therefore, if the hypotheses are correct it gives the exact solution. Nevertheless, it has not been mathematically proved, and its validity will be tested by comparison with analytical results obtained by the time-cone method in the available cases.

Equations (2.25) and (2.42) are the main results of this paper because they establish a simple way to calculate $C_1(r, t)$ and, in their turn, all the system autocorrelation functions as a function of the droplet size distribution function.

III. RESULTS

We have tested our method for the two typical more important cases given by the literature: the p -state Johnson-Mehl model (p -JM model) and the p -state cell model (p -cell model). The p -JM model considers constant nucleation frequency and constant isotropic growth rate for a

p -degenerated state. The p -cell model considers instantaneous nucleation restricted to the initial time ($t=0$) and constant and isotropic growth rate. In both cases, the time dependent particle size populations are evaluated by means of the ‘‘populational KJMA’’ model [8]. The resulting correlation functions are compared with those obtained by Ohta *et al.* [12], who used the time-cone method. In order to allow comparison between the two methods the nucleation radius, which cannot exist in the time-cone method but is inherent to the populational KJMA method, has been taken in the last case small enough, so that its effect becomes negligible. Furthermore, the method is applied to a kinetics characterized by diffusion controlled growth. Two cases are considered; namely, hard and soft impingement. The first is typical of stoichiometric compounds, assuming that there is no overlapping of the diffusion fields between growing grains, while the second appears in partitioning transformations, and takes into account the overlapping of the diffusion fields between contiguous grains. In all cases, the time dependent particle size distributions used for the evaluation of the correlation functions are obtained by means of the populational KJMA model [10,9]. In the case of a diffusion controlled growth, the correlation functions have not been calculated in the literature. Moreover, in the case of soft impingement, the time-cone method cannot be applied because the growth rate depends on the already crystallized fraction.

The time dependent particle size distributions evaluated by means of the populational KJMA model, and from which the correlation functions are obtained, are also given in the results. The grain size distributions are given in the form $n(r_0) = n(0 < r < r_0)$. Thus, the grain density ρ is defined as

$$\rho(r) = \frac{dn(r)}{dr}. \quad (3.1)$$

The p -JM and the p -cell models have been calculated in two and three dimensions. The calculations are not valid for one dimension because of the special characteristics of such a system, as Axe and Yamada [17] demonstrated. The cases of diffusion controlled growth have only been calculated in three dimensions for both hard and soft impingement, since it is a situation of major physical significance.

A. p -JM model

The p -JM model considered has a constant nucleation rate I and an isotropic droplet front velocity G . That is to say,

$$I(t) = I_0, \quad (3.2)$$

$$G(t) = G_0.$$

A nondimensional representation is chosen following [12], in which the natural time scale τ , length scale ξ , and density scale η are given by

$$\begin{aligned}\tau &= (I_0 G_0^D)^{-1/(D+1)}, \\ \xi &= \left(\frac{I_0}{G_0} \right)^{-1/(D+1)}, \\ \eta &= \xi^{-(D+1)} = \left(\frac{I_0}{G_0} \right).\end{aligned}\quad (3.3)$$

The results obtained for a two-dimensional and a three-dimensional system are shown in Figs. 1 and 2, respectively. Figures 1(a) and 2(a) show the dependence of the transformed fraction with time. The computed droplet size distributions, used in the evaluation of the correlation functions at different times, are shown in Figs. 1(b) and 2(b). In order to help comparison, the values of time selected are the same as those chosen by Ohta *et al.* [12], namely, $t/\tau = 0.25, 0.5, 0.75, 1, 1.25, 1.5,$ and 2 . Figures 1(c) and 2(c) show the autocorrelation functions $C_1^0(r,t)$ (dashed line) and $C_1(r,t)$ (solid line). The correlation functions, $C_0(r,t)$ and $G_0(r,t)$ are also shown in Figs. 1(d,e) and 2(d,e). Graphs for the rest of the correlation functions, $H_0(r,t)$, $H_1(r,t)$, and $G_1(r,t)$, are not shown, but they can easily be built up from the $C_1(r,t)$ function.

The particle size distribution shows a flat profile in both cases. Comparison with the results given by Ohta *et al.* shows that $C_1^0(r,t)$ is far from the exact result while $C_1(r,t)$ is very close. Differences are about 1% but they are not due to numerical approximations in our calculation but to the fact that we consider nuclei of finite size. This implies that the values of $\phi_0(t)$ are slightly different from those obtained by the time-cone method at the same times and, therefore, the numerical asymptotic values of the functions at the same times have to be different. However, both the correlation functions calculated with our method and with the time-cone method satisfy the analytical asymptotic behaviors summarized in Tables I and II. These results show the validity of the relationship between the correlation functions deduced in this paper.

B. p -cell model

For the p -cell model the nucleation events are restricted to $t=0$ and the droplet growth rate is constant and isotropic. That is to say,

$$\begin{aligned}I(t) &= I_0 \delta(t), \\ G(t) &= G_0.\end{aligned}\quad (3.4)$$

The natural time scale τ , length scale ξ , and density scale η are given by

$$\begin{aligned}\tau &= \frac{I_0^{-1/D}}{G_0}, \\ \xi &= I_0^{-1/D}, \\ \eta &= \xi^{-(D+1)} = I_0^{(D+1)/D}.\end{aligned}\quad (3.5)$$

Figures 3 and 4 show respectively the two-dimensional and three-dimensional cases. As in the previous case, the transformed fraction versus time (a), droplet size distribu-

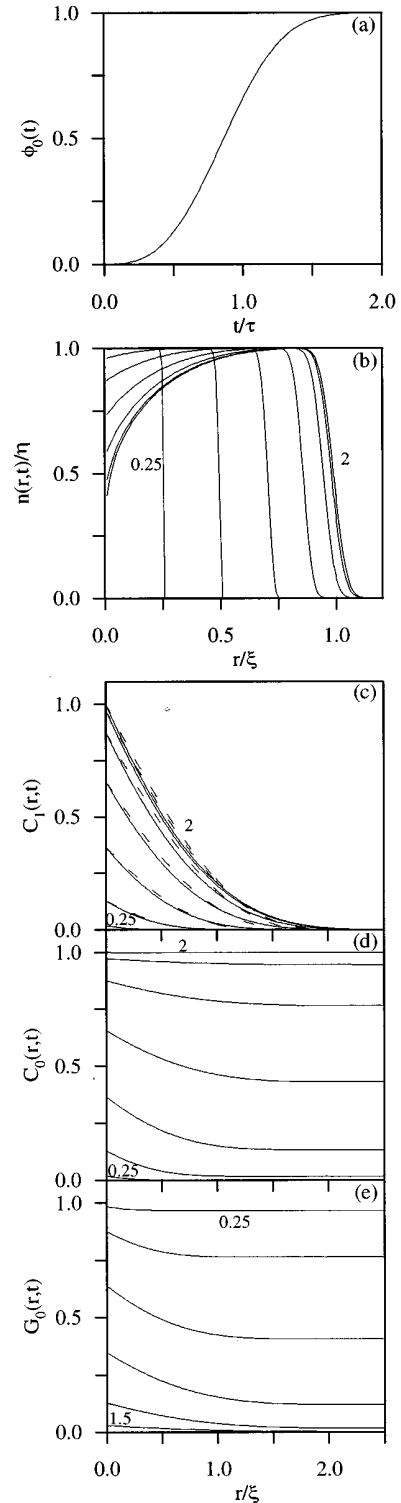


FIG. 1. Two-dimensional p -JM kinetics. (a) Transformed fraction vs time. (b) Computed droplet size distributions. (c) Autocorrelation functions $C_1^0(r,t)$ (dashed line) and $C_1(r,t)$ (solid line). (d) Correlation function $C_0(r,t)$. (e) Correlation function $G_0(r,t)$. (b)–(e) are plotted at $t/\tau = 0.25, 0.5, 0.75, 1, 1.25, 1.5,$ and 2 .

tions (b), correlation functions $C_1^0(r,t)$ and $C_1(r,t)$ (c), $C_0(r,t)$ (d), and $G_0(r,t)$ (e) are presented, at the same times chosen by Ohta *et al.*

A peaked profile is obtained in the droplet size distribu-

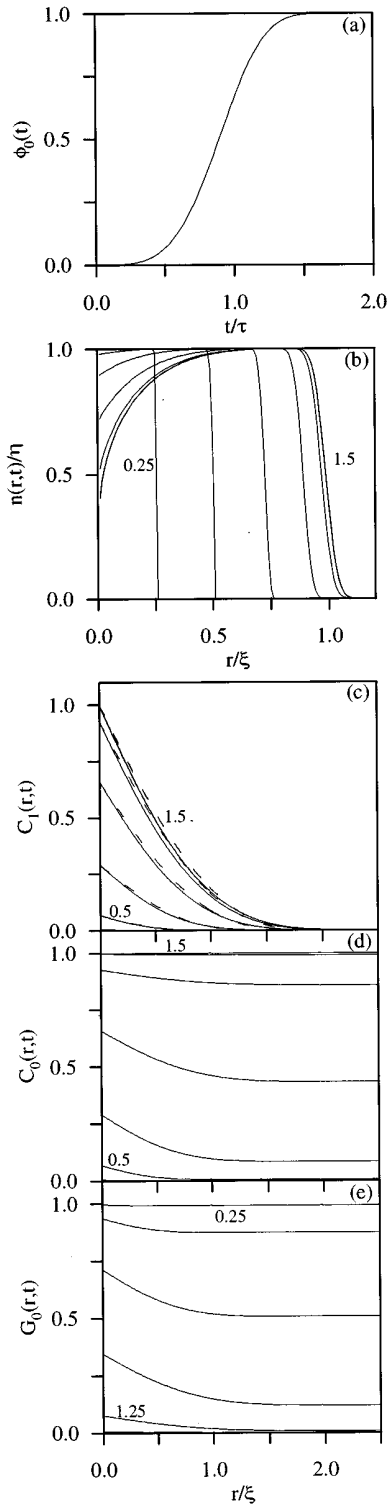


FIG. 2. Three-dimensional p -JM kinetics. (a) Transformed fraction vs time. (b) Computed droplet size distributions. (c) Autocorrelation functions $C_1^0(r,t)$ (dashed line) and $C_1(r,t)$ (solid line). (d) Correlation function $C_0(r,t)$. (e) Correlation function $G_0(r,t)$. (b)–(e) are plotted at $t/\tau=0.25, 0.5, 0.75, 1, 1.25$, and 1.5 .

tion, which is completely different from that obtained in the p -JM case. Consequently, a much more homogeneous grain distribution is obtained, which results in a shorter correlation length. Therefore, the fact that the final distribution has a small standard deviation around the average radius is re-

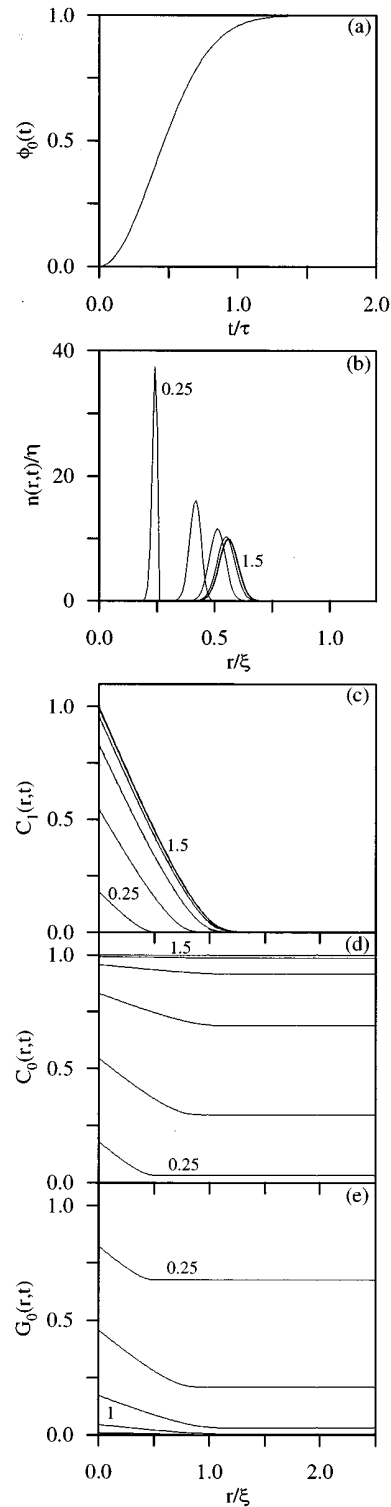


FIG. 3. Two-dimensional p -cell kinetics. (a) Transformed fraction vs time. (b) Computed droplet size distributions. (c) Autocorrelation functions $C_1^0(r,t)$ (dashed line) and $C_1(r,t)$ (solid line). (d) Correlation function $C_0(r,t)$. (e) Correlation function $G_0(r,t)$. (b)–(e) are plotted at $t/\tau=0.25, 0.5, 0.75, 1, 1.25$, and 1.5 .

flected in the correlation functions $C_1^0(r,t)$ and $C_1(r,t)$, which become much closer.

Comparison with the analytical time-cone results has also been performed and the same considerations given for the p -JM model apply.

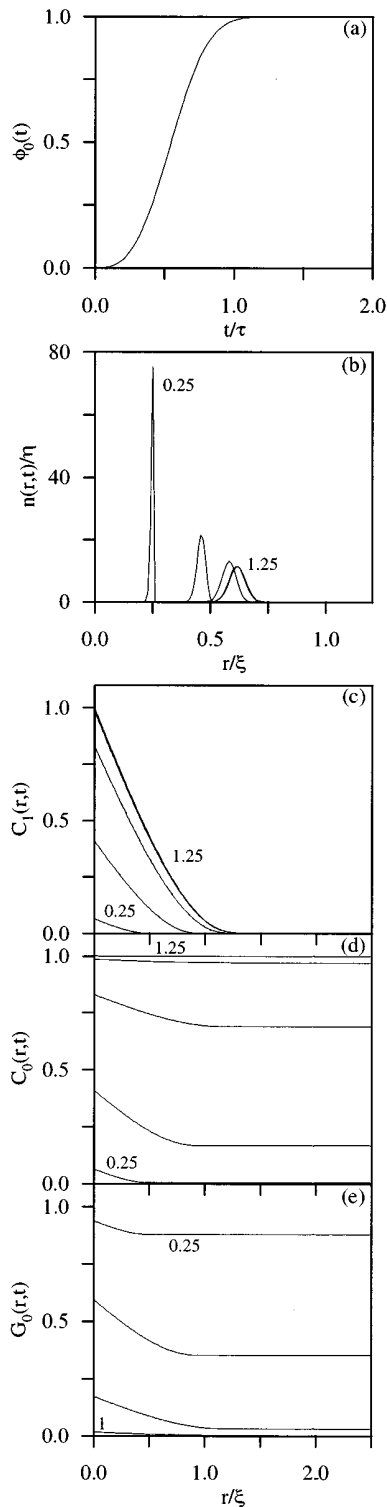


FIG. 4. Three-dimensional p -cell kinetics. (a) Transformed fraction vs time. (b) Computed droplet size distributions. (c) Autocorrelation functions $C_1^0(r,t)$ (dashed line) and $C_1(r,t)$ (solid line). (d) Correlation function $C_0(r,t)$. (e) Correlation function $G_0(r,t)$. (b)–(e) are plotted at $t/\tau=0.25, 0.5, 0.75, 1$, and 1.25 .

C. Diffusion controlled growth

Most of the interesting transformations driven by a nucleation and growth kinetics are primary precipitates with a composition differing from the original composition of the

material. These transformations result in a partially crystallized material, with a final crystallized fraction $\gamma=1-\phi_0(\infty)$. A diffusion controlled growth is normally obtained in such cases as a result of the migration of elements out of or into the newly formed crystals. The classical expression for the growth rate is obtained by considering a grain growing in isolation with spherical symmetry [18]. In this case, a steady-state concentration profile is obtained by taking the moving surface of the particle as the origin of the coordinates. The growth rate is given by

$$\frac{dr}{dt} = \tilde{D} \frac{C^* - C_0}{C^* - C_{xt}} \frac{1}{r}, \quad (3.6)$$

where C^* is the concentration of species at the surface of the particle, C_{xt} is that inside the crystal, and C_0 is that in the matrix far away from the particle. In this case, the droplet growth rate is isotropic but radius dependent, $G(R)$.

Moreover, a constant nucleation rate I_0 will also be considered. In this case, a particle growing in isolation is considered, and therefore there is no interference between the concentration profiles of different grains. This case is called diffusion controlled growth with hard impingement. We will perform the calculations assuming that the transformed fraction at the end of the primary precipitation is 50%, thus $\gamma=0.5$.

The natural time scale τ , length scale ξ , and density scale η are given by

$$\tau = (I_0 D_0^{D/2})^{-1/(D/2+1)},$$

$$\xi = \left(\frac{D_0}{I_0} \right)^{1/(D+2)}, \quad (3.7)$$

$$\eta = \xi^{-(D+1)} = \left(\frac{D_0}{I_0} \right)^{-(D+1)/(D+2)},$$

where

$$D_0 = \tilde{D} \frac{C^* - C_0}{C^* - C_{xt}}. \quad (3.8)$$

As in the previous case, Fig. 5 shows the transformed fraction versus time (a), droplet size distribution (b), correlation functions $C_1^0(r,t)$ and $C_1(r,t)$ (c), $C_0(r,t)$ (d), and $G_0(r,t)$ (e). The values of dimensionless time are the same as in the previous cases, showing that the characteristic dimensionless transformation time is of the same order of magnitude.

The droplet size distribution shows an asymmetrically peaked shape, very different from that obtained with interface controlled growth (p -JM kinetics). The correlation functions have shorter correlation lengths, much closer to the value found with the p -cell model. The value of $C_1(0,\infty)$ is, as expected, equal to the final transformed fraction, in our case taken to be 0.5.

In partitioning transformations, the overlapping between the concentration fields of neighbor grains cannot be avoided. In fact, this interference diminishes the concentration gradient at the surface of the grain, which results in a reduction of the growth velocity. This mechanism is known

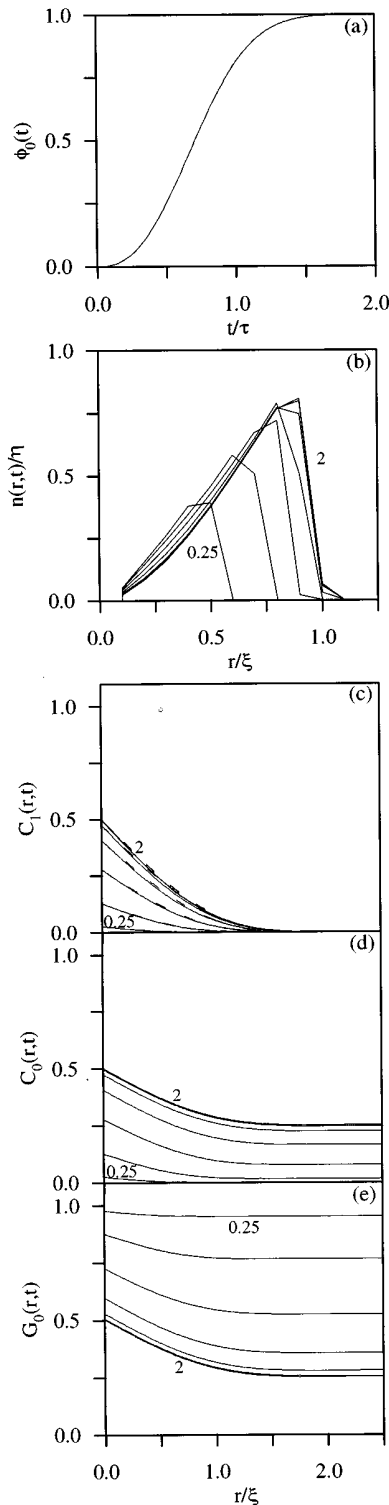


FIG. 5. Three-dimensional constant nucleation and diffusion controlled growth kinetics with hard impingement. (a) Transformed fraction vs time. (b) Computed droplet size distributions. (c) Auto-correlation functions $C_1^0(r,t)$ (dashed line) and $C_1(r,t)$ (solid line). (d) Correlation function $C_0(r,t)$. (e) Correlation function $G_0(r,t)$. (b)–(e) are plotted at $t/\tau=0.25, 0.5, 0.75, 1, 1.25, 1.5,$ and 2 .

as diffusion controlled growth with soft impingement. This fact may be taken into account by considering that the concentration of diffusing species far away from the grain has a mean value that increases as the transformation proceeds. By

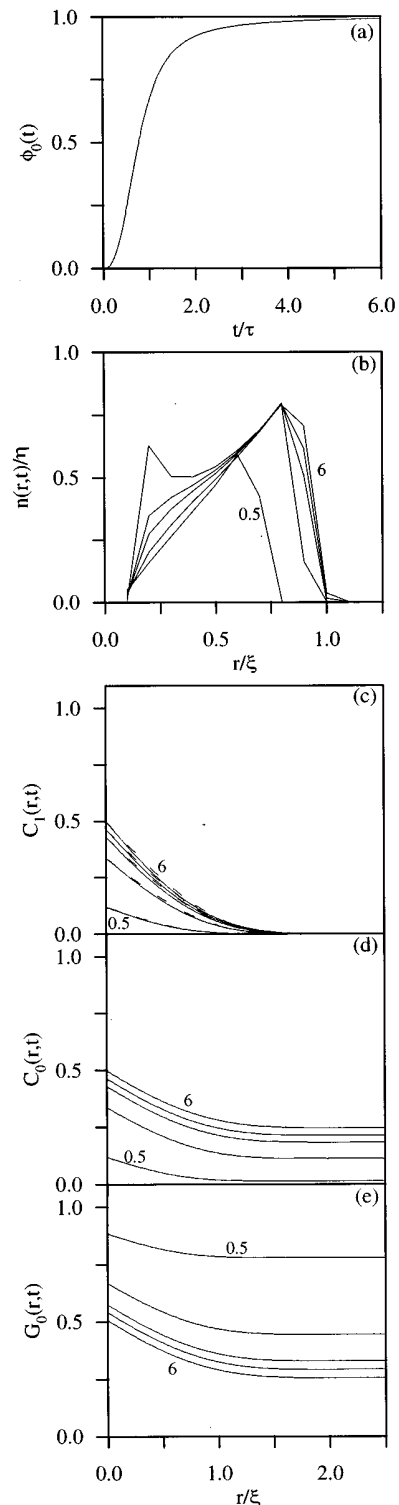


FIG. 6. Three-dimensional constant nucleation and diffusion controlled growth kinetics with soft impingement. (a) Transformed fraction vs time. (b) Computed droplet size distributions. (c) Auto-correlation functions $C_1^0(r,t)$ (dashed line) and $C_1(r,t)$ (solid line). (d) Correlation function $C_0(r,t)$. (e) Correlation function $G_0(r,t)$. (b)–(e) are plotted at $t/\tau=0.5, 1, 1.5, 2$ and 6 .

stating a mass balance of the diffusing species, and assuming that at the end of the transformation the concentration gradient disappears [10], a modification of the growth velocity is obtained:

$$\frac{dr}{dt} = \tilde{D} \frac{C^* - C_0}{C^* - C_{xt}} \left(\frac{1 - X(t)/\gamma}{1 - X(t)} \right) \frac{1}{r}, \quad (3.9)$$

where the concentrations are the same as in the case of hard impingement, and $X(t) = 1 - \phi_0(t)$ is the transformed fraction at time t .

The natural scales used for presenting the plots are the same as in the case of hard impingement. Figure 6 shows the transformed fraction versus time (a), droplet size distribution (b), correlation functions $C_1^0(r, t)$ and $C_1(r, t)$ (c), $C_0(r, t)$ (d), and $G_0(r, t)$ (e).

The droplet size distribution also shows an asymmetrically peaked shape, similar to that obtained for hard diffusion, the main difference being the accumulation of grains with small radii at the end of the transformation due to the reduced growth at large transformed fractions. Although the final shape is similar, the time dependence is completely different, showing that the soft impingement kinetics heavily delays the transformation with respect to hard impingement. This is also noted in the dimensionless time values, which are now $t/\tau = 0.5, 1, 1.5, 2,$ and 6 . The correlation functions also show a very different time dependence.

IV. CONCLUSIONS

The general relationship between spatial correlation functions and droplet size distribution is presented. This expression allows us to obtain all the correlation functions for a given microstructure for an arbitrary value of the degeneracy parameter p .

While considering nucleation and growth kinetics, exact correlation functions are obtained in the case of isotropic growth. The concept of isotropy in the growth rate includes the case where, with the growth of the droplets being an

anisotropic function, the spatial orientation of the growing droplets is still isotropic. In those cases, the hypothesis of self-similarity of the growing droplets enables us to obtain exact correlation functions, although the exact droplet size-shape distribution function still remains unknown.

The calculation of the correlation functions is performed by using the particle size distribution obtained by a recently developed model (populational KJMA). Since this model is less restrictive than those used in previously existing theories, the result is that the correlation functions can be obtained for dependencies of the kinetic magnitudes on time, crystallized fraction and the radius of the growing grain, and allows us to consider the finite size of the nuclei.

The method has been tested with the p -cell and p -JM models, for which exact correlation functions exist in the literature obtained by means of the time-cone method, and shows full agreement considering that in our calculations the finite size of the nuclei has been taken into account. Finally, the correlation functions corresponding to the microstructure developed in partitioning transformations, considering diffusion controlled growth with hard and soft impingement, are also obtained.

The use of the populational KJMA model for determining the particle size distributions, together with the method presented here for evaluating the correlation functions, results in a powerful tool in the evaluation of micro and macro properties of materials underlying first-order phase transitions.

ACKNOWLEDGMENTS

The authors wish to thank Dr. T. Pradell for her many helpful comments and her critical reading of the final manuscript. This work was partially financed by DGICYT, Grant PB94-1209, Generalitat de Catalunya 1997SGR 00039 and UPC, Grant PR9505.

-
- [1] A. N. Kolmogorov, *Bull. Acad. Sci. USSR, Phys. Ser.* **1**, 355 (1937).
- [2] W. A. Johnson and P. A. Mehl, *Trans. Am. Inst. Min. Metall. Pet. Eng.* **135**, 416 (1939).
- [3] M. Avrami, *J. Chem. Phys.* **7**, 1103 (1939).
- [4] M. Avrami, *J. Chem. Phys.* **8**, 212 (1940).
- [5] M. Avrami, *J. Chem. Phys.* **177**, 1941.
- [6] C. D. Van Siclen, *Phys. Rev. B* **54**, 11845 (1996).
- [7] V. Sessa, M. Fanfoni, and M. Tomellini, *Phys. Rev. B* **54**, 836 (1996).
- [8] D. Crespo and T. Pradell, *Phys. Rev. B* **54**, 3101 (1996).
- [9] D. Crespo, T. Pradell, M. T. Clavaguera-Mora, and N. Clavaguera, *Mater. Sci. Eng. A* (to be published).
- [10] D. Crespo, T. Pradell, M. T. Clavaguera-Mora, and N. Clavaguera, *Phys. Rev. B* **55**, 3435 (1997).
- [11] O. Glatter, *J. Appl. Crystallogr.* **13**, 7 (1980).
- [12] S. Ohta, T. Ohta, and K. Kawasaki, *Physica A* **140**, 478 (1987).
- [13] K. Sekimoto, *Phys. Lett.* **105A**, 390 (1984).
- [14] K. Sekimoto, *Physica A* **135**, 328 (1986).
- [15] K. Sekimoto, *Int. J. Mod. Phys. B* **5**, 1843 (1991).
- [16] K. Sekimoto, *J. Phys. Soc. Jpn.* **53**, 2545 (1984).
- [17] J. D. Axe and Y. Yamada, *Phys. Rev. B* **34**, 1599 (1986).
- [18] J. W. Christian, *The Theory of Transformations in Metals and Alloys* (Pergamon Press, Oxford, 1975).